37. Indykator tysku dlia vohnehasnyka: Pat. No. 6956 S1 UA. G 01 L 7/00 / Voropaiev V. M., Zhylin O. M., Plaksov S. V., Plotnikov V. V. No. 94061590; declareted: 16.06.1993; published: 31.03.1995, Bul. No. 1. 3 p.
38. Preobrazhenskiy V. P. Teplotekhnicheskie izmereniya i pribory. Moscow: Energiya, 1978. 704 p.
39. Zlotnikov V. O., Popovych O. V., Kushchevskyi M. O. Prystriyi dlia vymiriuvannia dynamichnoho tysku zatoplenoho hidro strumenia: Pat. No. 55669 UA. G01L 7/00. No. u201000403; declareted: 18.01.2010; published: 10.09.2010, Bul. No. 17. 3 p.
40. Yakymchuk O. V., Sidletskyi I. O., Kushchevskyi M. O. Pro vplyv heometrychnykh parametriv nasadkiv ta zatoplenoho hidrostrumenia na yakist formuvannia obiemnykh detalei holovnykh uboriv // Visnyk Zhytomyrskoho derzhavnoho tekhnolohichnoho universytetu. 2010. Issue 2. P. 61–67.

UDC 621.914
DOI: 10.15587/1729-4061.2018.121712

MODELLING THE LOADING OF THE NOSE-FREE CUTTING EDGES OF FACE MILL WITH A SPIRAL-STEPPED ARRANGEMENT OF INSERTS

L. Hlembotska
Assistant*
E-mail: gle.tmkts@gmail.com
P. Melnychuk
Doctor of Technical Sciences, Professor**
E-mail: meln_pp@ukr.net
N. Balytska
PhD**
E-mail: balytskanataliia@gmail.com
O. Melnyk
PhD*
E-mail: o.l.melnyk@ukr.net
*Department of branch of Machine Building***
Department of Applied Mechanics and Computer-Integrated Technologies*
***Zhytomyr State Technological University
Chudnivska str., 103, Zhytomyr, Ukraine, 10005

Розглянуто задачу аналітичного визначення завантаженості безвершинних різальних кромок торцевої фрези зі спірально-ступінчастим розташуванням ножів. Розроблено математичну модель визначення елементів зрізу в довільному положенні ножів фрези на дузі контакту, достовірність якої підтверджена імітаційним моделюванням. Виявлено залежності величини елементів зрізу від конструктивних параметрів фрези та подачі

Ключові слова: торцеве фрезерування, елементи зрізу, ступінчасті схеми різання

Рассмотрена задача аналитического определения загруженности безвершинных режущих кромок торцевой фрезы со спирально-ступенчатым расположением ножей. Разработана математическая модель определения элементов среза в произвольном положении ножей фрезы на дуге контакта, достоверность которой подтверждена имитационным моделированием. Выявлены зависимости величины элементов среза от конструктивных параметров фрезы и подачи

Ключевые слова: торцевое фрезерование, элементы среза, ступенчатые схемы резания

1. Introduction

Face mills are widely used both in roughing, semi-finishing and finishing of flat surfaces of machine parts. Raising the productivity of milling such surfaces is an acute problem of modern machine building and can be achieved by increasing feed and/or cutting rate. In turn, intensification of cutting rate necessitates the use of super-hard tool materials which dramatically increases machining costs, especially for multi-toothed tools. Besides, rise of cutting modes worsens dynamic state of the technological processing system and limits the possibility of improvement of machining productivity. Therefore, it is necessary to develop advanced designs of face mills characterized by a better dynamic stability of the machining process, calculated for machining conditions with larger feeds and providing required surface quality. These include mills with spiral-stepped cutting schemes having nose-free cutting edges and featuring different cut areas for different inserts.

The decision on appropriateness of using a tool of a particular design cannot be made without analysis of peculiarities of its cutting edge loading. The process of face milling is characterized by impacts occurring at the entrance/exit of the insert to/from the cutting zone, variability of the chip thickness along the contact arc, the number of inserts that are simultaneously involved in the cutting process and so on. All this brings about significant periodic fluctuations of cutting forces affecting quality of the machined surface, tool durability, dynamic state of the entire technological processing system. Calculation of cutting forces is based on predetermined elements of the cut. While definition of these parameters for standard mills working by a generator cutting scheme is not difficult, this problem remains unresolved for the face mills working by spiral-stepped cutting schemes and having nose-free cutting edges. Therefore, analytical determination of the cut elements along the entire tool/workpiece contact arc is required for each insert of the face mill under study. From a practical point of view, the developed mathematical model will make it possible to determine rational values of feed and structural parameters of the face mill for its effective operation at various depths of cut.

Thus, the applied aspect of using the obtained scientific result is the possibility of raising productivity of machining flat surfaces while providing required quality which determines relevance of this study.

2. Literature review and problem statement

One of the lines of development in modern machine-building industry is raise of machining productivity. At the same time, it is important that quality of the machined surfaces is preserved. Required surface roughness can only be achieved at satisfactory dynamic characteristics of the technological processing system during the cutting process.

An important contribution to the study of stability of the milling process was made in [1] but the proposed analytical model does not take into account cut distribution for stepped face mills and the geometric parameters of the tool.

A mathematical model for determining cutting forces acting in machining with face mills having round inserts made of cutting ceramics has been developed in work [2]. This model allows one to determine optimal geometric parameters of inserts to provide improved processing performance by predicting dynamic characteristics of the cutting process. However, this study is aimed at improvement of productivity by increasing cutting speed only and therefore it cannot be applied for stepped hard-alloy face mills.

Study [3] is devoted to determining dynamic characteristics of cutting with the use of stepped face mills and mills of a standard design. In this case, the mathematical model of dynamics of the face milling process is based on the refining coefficients taking into account properties of the processed material, parameters of the cutting mode and geometry of the cutting part of the tool. However, choice of these coefficients is rather limited and conditional.

Dependence of the roughness parameters of machined surfaces on geometric parameters of the tool was considered in [4–6]. The results obtained in [4, 5] show high efficiency of use of both plaining cutters and face mills with a cylindrical front surface of inserts when machining parts at large feeds.

The authors of paper [6] studied dependence of machined surface quality on geometric parameters of the face mills in high-speed machining. Geometric model of prediction of the machined surface roughness is only oriented on the cutting process with square inserts and therefore cannot be used in this study.

The authors of papers [5, 7, 8] studied influence of milling modes on the machined surface quality. The issues of optimization of cutting modes in finishing flat surfaces of the parts made of hard-to-work materials using stepped mills of super-hard materials were solved in [5]. However, a purely experimental approach does not allow one to apply the obtained results in roughing and semi-finishing using hard-alloy stepped face mills with other cutting schemes. Effect of the cutting speed alone on roughness of the surface subjected to face milling was investigated in [7].

The method of fractal analysis was used in [8] to describe microrelief of the surface formed by face milling at various feed magnitudes. However, this study is aimed at standard face mills and does not solve the problem of raising productivity of milling flat surfaces.

It should be noted that the common feature of all above-mentioned works is their orientation to machining with standard face mills with a generator cutting scheme characterized by worsening of dynamic characteristics of the machining process when feed and cutting speed are intensified. At the same time, in accordance with [3, 9, 10], face mills with combined cutting schemes have a higher level of dynamic stability compared with the standard mills.

The authors of studies [5, 11, 12] solved the problem of raising productivity of machining flat surfaces thru working out advanced mill designs using stepped cutting schemes of various types. The most common is Archimedes' spiral [11] and logarithmic spiral [12] arrangement of inserts.

As is known, Archimedes' spirals are characterized by a constant radial step of the turns on which inserts are positioned. This results in a constant width but a growing thickness of each chip cut by the inserts with enlarged main cutting edge angle. Radial distance between the turns in the logarithmic spiral increases indefinitely which overloads roughing inserts. Therefore, in order to reduce chip thickness and width of the roughing insert cut, it is advisable to use the Fermat's spiral in which the radial step of turns decreases in the direction from the center [5].

The works [11, 13] are characterized by the use of cutting inserts with flat front and cylindrical rear surfaces, setting of various insert height above the surface of the end mill body and obtaining of the overall cutting surface of a conical shape. Analysis of these cutting schemes shows that because of the large difference in cutting speeds of individual inserts (especially between the inserts on smaller and larger diameters), they materially differ in their wear. Because of small cutting edge angles, growth of the copying phenomenon is observed for roughing inserts. In addition, because of the large difference in the diameters on which the first and last inserts are positioned, the width of the workpiece is limited and/or an increase in the mill size is observed.

In work [5], it is proposed to form the general cutting surface of a toroidal shape by giving toroidal shape to the face mill body. The insert that cuts the outer surface of the workpiece is characterized by a cutting edge angle close to the right angle which determines minimum copying of the workpiece surface on the part surface. The insert that cuts the inner surface of the part has a zero cutting edge angle. Due to such positioning of inserts on the torus circle, the finishing insert cuts small thickness, which ensures high quality of the surface layer.

Also, works [14–16] propose to use inserts with an arc-shaped cutting edge which results in an increased length of the active section of the cutting edge, improved quality of the machined surface and higher milling productivity.

Authors of paper [5] propose the design of the face mill with cylindrical front and flat back surfaces of the inserts positioned on the sections of the Fermi spiral on a toroidal body which ensures higher productivity and quality of the machined surface. It was established that when machining flat surfaces with a spiral-stepped face mill having cylindrical front surface of inserts, productivity is 2.9 times higher compared with grinding. In this case, roughness of the machined surface R_a=1.2 µm and deviation from flatness Δ=25 µm were ensured. However, the cut elements remain uncertain for mills of this design which makes it impossible to analyze the insert loading and further calculation of the cutting forces under various milling conditions. Therefore, for scientific substantiation of the insert loading in the mill proposed in [5], it is necessary to develop a mathematical model in order to determine the cut elements for inserts of all machining steps.

3. The aim and objectives of the study

This study objective was to construct a mathematical model of loading the nose-free face mill cutting edges with a spiral-stepped arrangement of inserts on a toroidal body. This will make it possible to determine the cut elements of each insert of the face mill under various machining conditions and formulate recommendations for the choice of rational structural parameters of the face mill for certain depths in cut.

To achieve this objective, the following tasks were set:

– determine analytically the chip thickness and width of cut, the depth of cut, the maximum cutting edge angle and the cut area for each insert of the face mill at an arbitrary point of the contact arc;

– check reliability of the developed mathematical model by means of simulating loading of the face mill cutting edges;

– based on the developed mathematical model, study influence of the design parameters of the face mill and the feed magnitude on the cut elements for each insert of the mill;

– formulate recommendations for assigning rational structural parameters to the face mill for certain depths of cut.

4. The procedure for determining loading of the cutting edges of the face mill

4. 1. Features of the face mill design

The design of the studied face mill with a spiral-stepped arrangement of inserts and nose-free cutting edges is shown in Fig. 1. When creating stepped cutting schemes, the inserts 5 are arranged on one or more spirals, and in the axial plane, they are turned around the circle axis 11 by the angles η_i relative to each other.

The total cutting surface is formed by radial arrangement of each insert on the body of the face mill and a relative turn of the axis of each insert round the torus axis by the angle η_i (Fig. 1).

In order to perform semi-finishing process (a depth of cut of 3 mm), it was proposed to place 12 inserts on the Fermat's spiral on the toroidal body of the face mill according to a stepped cutting scheme (3 sites of 4 inserts) with a uniform angular step between the inserts (angle θ). Diameter of the mill: 160 mm (behind the insert positioned on the minimum diameter); diameter of the inserts: 10.8 mm; slope of the cutting assemblies: –6, 0, 6, 12°; clearance angle: 16°.

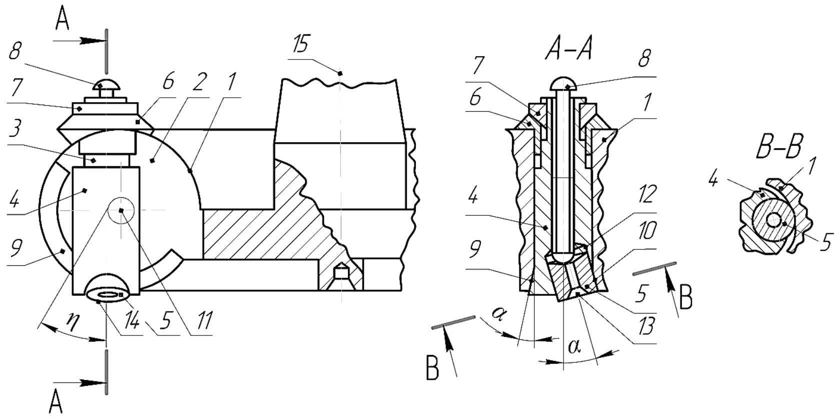

Fig. 1. The design of the face mill: toroidal body (1); axial groove (2); cutter assembly (3); holder (4), round insert (5), washer (6); nut (7); adjusting screw (8); chamfers (9, 10); circle axis (11); cylindrical hole under the insert (12); insert axis (13); end edge of the insert (14); axis of the face mill (15)

4. 2. Methods applied in modeling the loading of cutting edges of the face mill

When constructing the mathematical model of loading the cutting edges of the face mill, the following assumptions were taken: no wear of the cutter inserts, no beating of inserts, shank, mandrel, spindle, etc., a uniform allowance for machining.

To calculate elements and chip thickness, it is necessary to use the Cartesian coordinate system as follows: *XOY* coincides with the cutting plane, *XOZ* coincides with the main plane, *YOZ* coincides with the secant plane. Axis *Z* coincides with the axis of rotation of the mill (Fig. 2, *a*). Projection of the rear flat surface of the insert on the main plane of the *XOZ* has the form of ellipse.

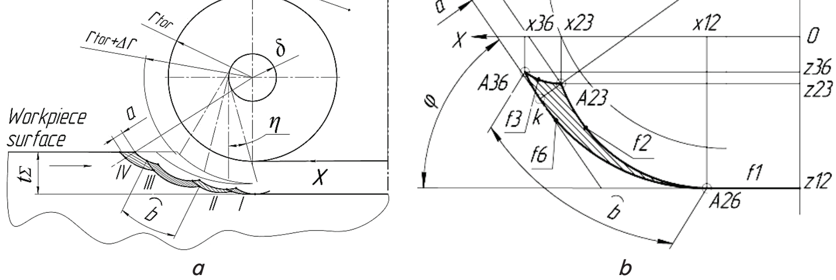

Fig. 2. Elements of the cut: *a* — cutting scheme; *b* — section of the insert cut in the first step

The shape of the cut made by each insert is determined by position of the cutting edges of adjacent inserts in the main plane *XOZ* (Fig. 2, *b*).

For mathematical modeling, it is necessary to enter initial data (Fig. 2): mill radius: *R*, torus radius: r_{tor}; insert radius: r_{ins}; clearance angle: α; displacement of the axis of the cutting assembly: δ; number of inserts: *k*; number of spirals: *N*; feed per minute: $f_{\min}$; spindle speed: *n*; travel of the center of the flat back surface of the insert: Δr; angle of slope of the cutting assembly axis relative the axis of the toroidal body of the mill: η_i.

Development of a mathematical model of loading of nose-free cutting edges of the inserts of the mill with a spiral-stepped cutting scheme was carried out in the following sequence.

1. Determination of the initial and final radii on which the inserts of the mill cutter are positioned in three sites of the Fermat's spiral:

$$\rho_{0,k} = R + \delta + \left(\sqrt{(r_{tor} + \Delta r)^2 - \delta^2} + \delta \cdot \mathrm{tg}\,\eta_i\right) \cdot \sin\eta_i. \quad (1)$$

2. Determination of coordinates of centers of the rear flat surface of cylindrical inserts on the *XOZ* plane:

$$x_i = \rho_i;$$
$$z_i = r_{tor} - \left(\sqrt{(r_{tor} + \Delta r)^2 - \delta^2} + \delta \cdot \mathrm{tg}\,\eta_i\right) \cdot \cos\eta_i, \quad (2)$$

where ρ_i is the radial distance of the center of the rear flat surface of each insert calculated using the Fermat's spiral equation.

3. Considering that the inserts of the proposed mill are positioned at various radial distances and at various slope angles η_i of each cutting assembly relative the mill axis, the canonical ellipse equation has the following form:

$$X^2 / r_{ins}^2 + Z^2 / \left(r_{ins} \cdot \sin\alpha\right)^2 = 1, \quad (3)$$

where

$$\begin{cases} X = (x - x_i) \cdot \cos\eta_i + (z - z_i) \cdot \sin\eta_i, \\ Z = -(x - x_i) \cdot \sin\eta_i + (z - z_i) \cdot \cos\eta_i \end{cases}$$

are the formulas for converting a new coordinate system to a *XOZ* coordinate system that takes into account transition of the coordinate system and the turn by the angle η_i.

4. Definition of general equations of projections of inserts (ellipses) on the main plane in the form:

$$Ax^2 + 2Bxz + Cz^2 + 2Dx + 2Ez + F = 0. \quad (4)$$

5. Finding coordinates of the points of intersection of the ellipses A12, A23, A36 (Fig. 2, *b*) by solving the system of equations:

$$\begin{cases} f_1(x,z), \\ f_2(x,z), \\ f_3(x,z), \\ f_4(x,z), \end{cases} \quad (5)$$

where $f_i(x,z)$ are general equations of the ellipses that form each cut.

6. Determination of maximum chip thickness *a*, width of cut *b*, maximum cutting edge angle φ, depth of cut *t* and cut area *S* for inserts of all steps is carried out in the following sequence (Fig. 2, *b*):

– equation of the straight line passing through the center of the torus O_{tor} and the intersection point A23 is determined;

– coordinates of intersection of the straight line and the ellipse are determined by solution of the system of equations:

$$\begin{cases} f_6(x,z), \\ z = kx + c; \end{cases} \quad (6)$$

– the chip thickness is determined by the formula:

$$a_i = \sqrt{\left(x_k - x_{ij}\right)^2 + \left(z_k - z_{ij}\right)^2}, \quad (7)$$

where x_k, z_k are coordinates of the point of intersection of the straight line and the ellipse (6); x_{ij}, z_{ij} are the coordinates of the point of intersection A23 of the corresponding ellipses;

– the maximum main cutting edge angle φ is determined at the studied point of the cutting edge x_{ij}, z_{ij}:

$$\varphi_i = \arcsin\left(\left(a_i \cdot n \cdot N\right) / f_{\min}\right); \quad (8)$$

– the depth of cut by the insert at each step is determined:

$$t_i = z_{36} - z_{12}, \quad (9)$$

where z_{36} and z_{12} are the coordinates of the points of intersection of the ellipses A36 and A12 that form the corresponding cut (Fig. 2, *b*);

– the width of cut is defined as the length of the arc which is the projection of the active section of the cutting edge at each step:

$$b_i = \int_{x_{12}}^{x_{26}} \sqrt{1 + \left(f(x)'\right)}, \quad (10)$$

where x_{36}, x_{12} are the boundary coordinates of the points of the arc (the width of the cut); $f(x)$ is the equation of the corresponding ellipse, which determines the width of cut;

– the area *S* of the cuts made by inserts in all steps is determined as the area of the curvilinear figure limited by arcs:

$$S_{ij} = \int_{x_{26}}^{x_{23}} \left(f_2(x) - f_6(x)\right) \mathrm{d}x + \int_{x_{23}}^{x_{36}} \left(f_3(x) - f_6(x)\right) \mathrm{d}x, \quad (11)$$

where x_{23}, x_{26}, x_{36} are the boundaries of integration, the coordinates of the points of intersection of the ellipses that form the corresponding cut.

The areas of the cuts made by inserts in each step of the cutter at an arbitrary point of the contact arc will be determined by the formula:

$$S_i = S_{ic} \cdot \cos\psi_i = S_{ic} \cdot \cos\left(\frac{B/2 \pm \varepsilon}{R_i}\right), \quad (12)$$

where S_{ic} is the area of the cut made by the insert in the corresponding step in the base plane (the main plane passing through the cutter axis and the direction of feed).

4. 3. Simulation of loading of the cutting edges of the face mill

The results of the conducted analytical study require an experimental verification. However, the cut elements cannot be measured directly because of the metal chip shrinkage. Determination of cutting elements by mediating methods does not provide sufficient accuracy. In view of this, to simulate adequacy of the developed mathematical model, simulation of loading of the cutting edges was performed in the SolidWorks Motion environment by graphic modeling of the mill and the workpiece motion. When doing this, due to drawing a sketch in the context of assembly and formation of projections of the cutting edges, flat figures (which are sections of the cut material) were obtained and their areas determined.

All elements that were insignificant for this study (e. g. fixtures of the cutting units) were excluded from the simulation model and the mutual positions of the parts of the model assembly were determined by the conjugations between the parts.

In order to perform simulation, a solid-state model has been created for the cutter and the workpiece assembly (Fig. 3, *a*). The design parameters of the mills correspond to the abovementioned ones, the milling width $B=82$ mm, the shift of the mill axis relative to the axis of symmetry of the workpiece $\varepsilon=10$ mm. The shift of the workpiece in the direction of cut-in of the insert of the face mill provides beginning of cutting at a reduced chip thickness.

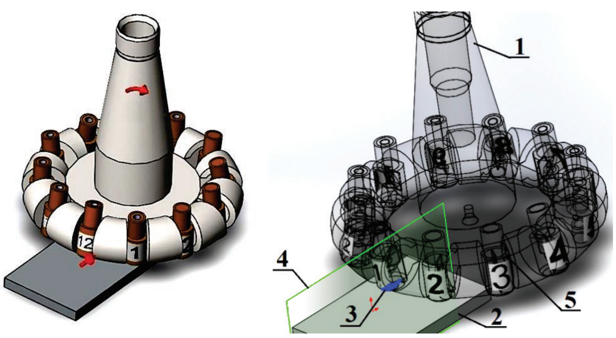

a *b*

Fig. 3. Solid-state model of the mill and the workpiece assembly: general view of the simulation model (*a*); the sketch of the model in the context of the assembly (*b*): the mill (1); the workpiece (2); the sketch of projections of the cutting edges (3); auxiliary plane (4); the cutter insert of an individual number (5)

Simulation of the mutual motion of the workpiece and the mill was realized by two motors: linear (simulating the workpiece feed) and rotary (simulating rotation of the mill). The speed of the linear motor was 1.33 mm/s (corresponding to the workpiece feed $f_{min}=80$ mm/min); spindle speed of the rotary motor was 200 rpm. In the parameters of motion study, 1500 frames per second was set at a study time of 0.15 seconds (the time for which the cutter makes 1/2 revolution). At the time moments of the study, when the centers of the rear surfaces of the cutter insert alternately coincided with the base plane (the main plane passing through the cutter axis and the feed direction), projections of the cutting edges on this plane were obtained (Fig. 4, *a*).

To determine the cut area, the resulting sketch was edited by cutting off extra elements to form the cut cross-section (Fig. 4, *b*). Based on the sketch geometry, SolidWorks software defined its area with a specified accuracy.

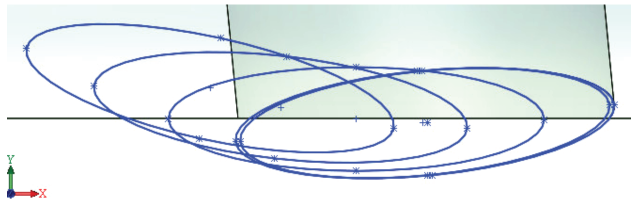

a

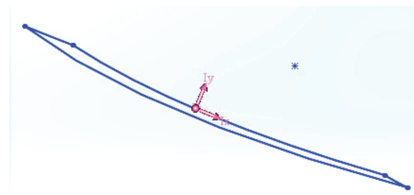

b

Fig. 4. Formation of a sketch by projection of cutting edges on the auxiliary plane: projections of the set of cutting edges (*a*); the cut form (*b*)

Fig. 5 shows a comparative diagram of the results of mathematical modeling and simulation of loading of nose-free cutting edges of the mill inserts with a spiral-stepped cutting scheme.

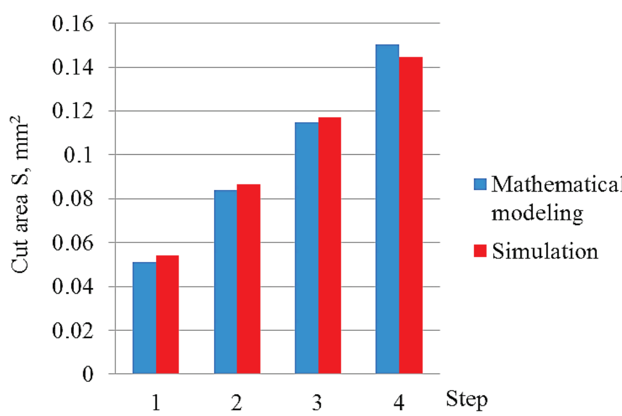

Fig. 5. Diagram of the results of calculating the cut area with the inserts of each step of the face mill in the main plane

Since the relative error in determining the area of cuts by mathematical modeling and simulation ranges from 1.8 % to 5.7 %, reliability of the mathematical model can be considered confirmed.

Based on the mathematical model, calculations were carried out in the Maple environment which has allowed us to determine size of the cut elements of each insert of the mill at an arbitrary point of the contact arc.

5. Results obtained in the simulation of loading of cutting edges of the face mill

Using the calculations made in the Maple environment, the effect of the design parameters of the face mill and the feed magnitude on the cut elements were studied. Simulation of loading of the cutting edges of the studied face mill was performed for the above-mentioned cutting conditions ($t=3$ mm, $B=82$ mm, $\varepsilon=10$ mm).

Graphic dependences obtained according to the results of calculations are shown in Fig. 6–8.

The results of simulation of the effect of the feed magnitude $f_{\min}$ on chip thickness, width of cut, depth of cut, maximum main cutting edge angle and the cut area for each insert of the mill are shown in Fig. 6

Fig. 7 shows the results of modeling the dependence of the cut elements for each insert of the mill on the value of the clearance angle.

The results of modeling the influence of the slope angles of the cutter assemblies of the face mill on the cut elements for each insert of the mill are shown in Fig. 8.

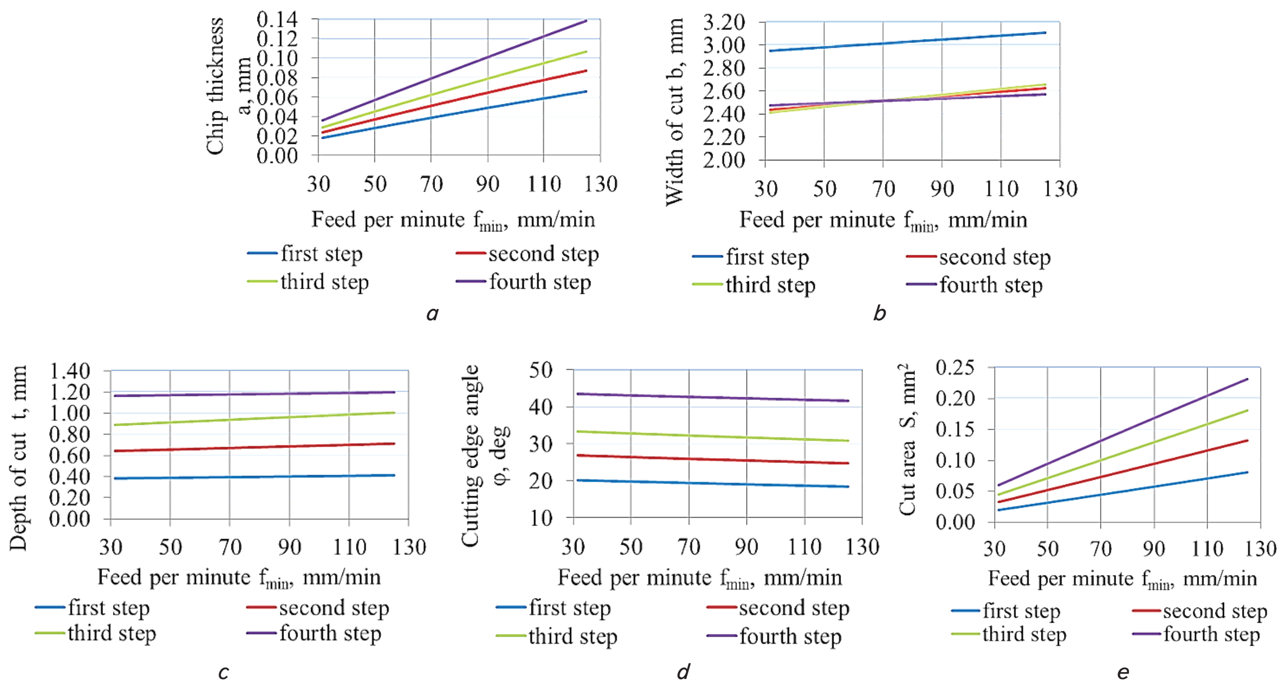

Fig. 6. Effect of the feed magnitude $f_{\min}$ on the cut elements for each insert of the mill: on the chip thickness (*a*); on the width of cut (*b*); on the depth of cut (*c*); on the main cutting edge angle (*d*); on the cut area (*e*), ($\alpha = 16°$, $\eta = -6, 0, 6, 12°$)

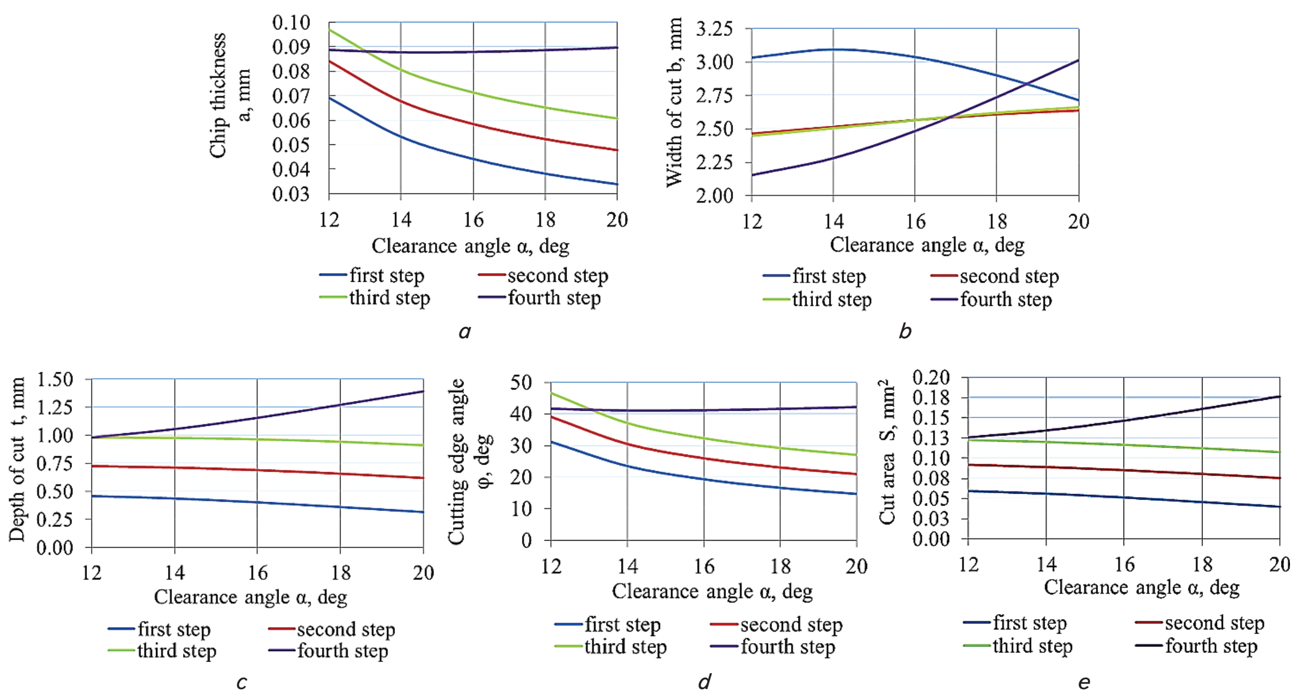

Fig. 7. Effect of the clearance angle value α on the elements of the cut for each insert of the cutter: on the chip thickness (*a*); on the width of cut (*b*); on the depth of cut (*c*); on the main cutting edge angle (*d*); on the cut area (*e*); ($f_{\min} = 80$ mm/min, $\eta = -6, 0, 6, 12°$)

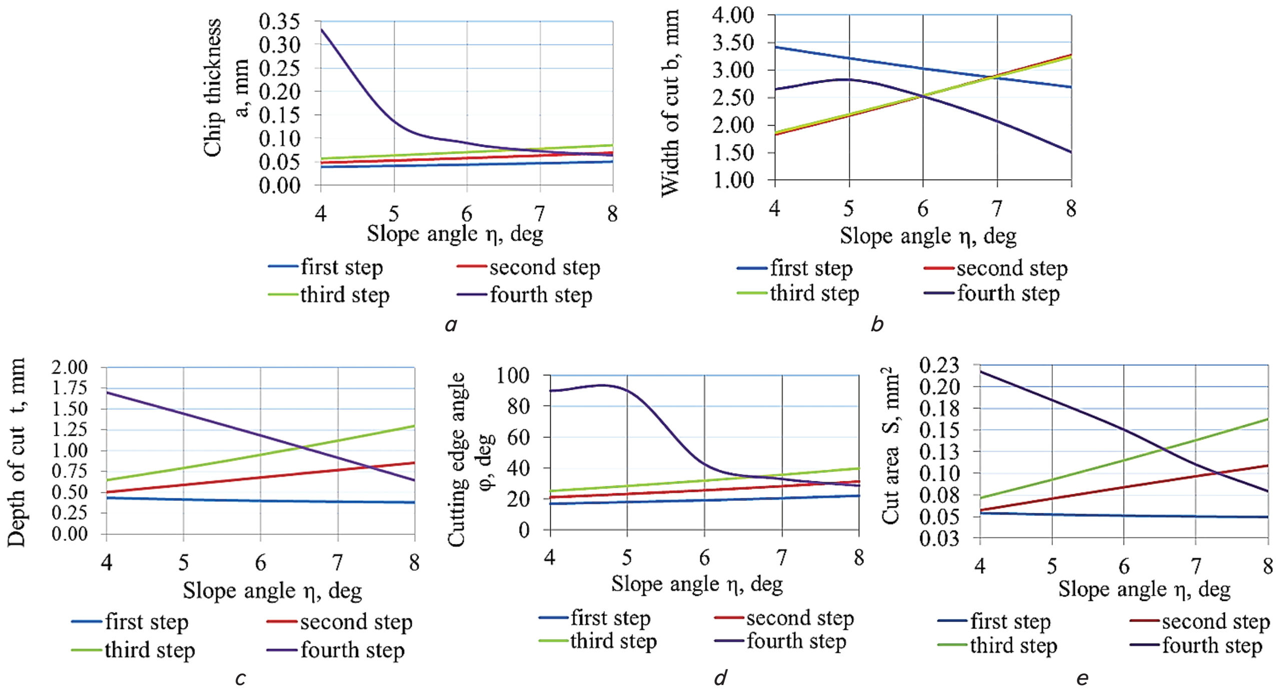

Fig. 8. Influence of angles η of slope of cutting assemblies on the elements of cut for each insert of the mill: on the chip thickness (*a*); on the width of cut (*b*); on the depth of cut (*c*); on the main cutting edge angle (*d*); on the cutting area (*e*) (f_{min} = 80 mm/min, α = 16°)

6. Discussion of the results obtained in the study of loading of the cutting edges of the face mill

The problem of mathematical description of loading of the face mill cutting edges with a spiral-stepped cutting scheme was solved analytically in absence of simplifications of any kind which results in a high accuracy of the results obtained and determines the value of this work.

Based on the results obtained, the following conclusions can be drawn. An increase in the feed magnitude caused linear increase in chip thickness and width of the cut and the depth of cut for inserts of all steps (Fig. 6). The chip thickness was most intensively increased and the depth of cut increased the least. It is consistent with the well-known provisions of the theory of cutting. In this case, the width of cut for inserts of the first step was the largest which determined improvement of quality of the machined surface formed by successive positions of the cutting edges of inserts of the very first step. It is also worth noting that the ratio of the width of cuts varied when the feed per minute of 70 mm/min was reached. At the same time, growth of feed caused linear reduction of the main cutting edge angle, at the point that corresponds to the largest chip thickness, with all angle values obtained in the plan being permissible (<90°). Change in the values of all these cut elements leads to a gradual linear increase in the cut area for the inserts at all steps of the face mill. Thus, in the whole range of changes of feed magnitude, the inserts of the fourth (roughing) step of the mill were most loaded and the inserts of the first (finishing) step were the least loaded.

As can be seen from Fig. 7, growth of the clearance angle from 12° to 20° caused gradual decrease in the chip thickness, the depth of cut and the main cutting edge angle for the inserts of all steps of the face mill except the fourth step. This result is explained by the fact that the elliptical projections of the cutting edges were characterized by a decrease in the size of the small semi-axis with the growth of the clearance angle which resulted in overloading of the fourth step. At the values of the clearance angle α<16°, the width of cut will increase from the roughing teeth to the finishing ones and at α>16°, this order was broken which is not rational. Such interconnections between the clearance angle and the elements of the cut caused a gradual decrease in the cut area for the inserts of all steps, except for the fourth (Fig. 7, *e*) with the growth of α_N.

Therefore, proceeding from the above, a conclusion can be drawn that it is expedient to assign angle of 16° to the face mill of the proposed design since it is in this case that the cut area for the inserts in various steps will grow uniformly from the first to the fourth step.

Graphic dependences (Fig. 8) indicate overload of inserts of the fourth step with a decrease in slope angles of the cutting assemblies to 4–5° with the magnitude of the main cutting edge angle exceeding the recommended values (<90°). At the same time, growth of these angles to 7–8° caused transfer of the maximum load on the inserts of the third or second step which is not expedient (Fig. 8, *e*).

Therefore, for the studied mill, at the condition of general machining depth of 3 mm, the assigned values of slope angles of the cutting assemblies of 6° can be recommended since in this case the cut area for the inserts in various steps will increase proportionally from the first step to the fourth. In the case of machining at larger depths of cuts, values of the angles of slope of the cutting assemblies should be increased and reduced at smaller depths of cuts.

The conducted study has made it possible to propose rational values of the basic design parameters of the face mill depending on the required depth of cut (Table 1).

Thus, for effective operation of the face mill of the studied design at the depth of cut of 3 mm, it is expedient to use

5.4 mm radius inserts, slope of the cutting assemblies of 6° and the clearance angle of 16°. If it is necessary to increase the total depth of cut, it is recommended to use inserts with larger angles of slope of the cutting assemblies and greater values of the clearance angle. This will make it possible to avoid overload of the inserts of the fourth step of the mill. And vice versa, at a smaller depth of cut, it is possible to use inserts with smaller angles of slope of the cutting assemblies and the clearance angle.

Table 1

Recommended values of design parameters of the face mill

Design parameters of the face mill	Depth of cut t, mm				
	2	2.5	3	3.5	4
Cutting assembly slope angle η_i, degrees	4	5	6	7	8
Clearance angle α, degrees	12	14	16	18	20

The obtained results can be used to improve productivity of machining flat surfaces while providing required quality through the use of the face mills with a spiral-stepped cutting schemes and nose-free cutting edges.

This study may be further improved by taking into account wear and beating of the face mill inserts and unevenness of machining allowances.

7. Conclusions

1. A mathematical model of loading of the cutting edges of each insert of the face mill with a spiral-stepped cutting scheme was created. It was established that the size of the cut elements depends on the feed magnitude, design parameters of the mill and the insert position on the contact arc. The variables of the mathematical model in this study included the feed magnitude, the clearance angle of the insert and the slope angle of the cutting assemblies. The developed model makes it possible to determine the chip thickness and width of cut, the depth of cut, the maximum value of the main cutting edge angle and the cut area at an arbitrary position of the mill insert on the contact arc.

2. Reliability of the developed mathematical model was confirmed by simulation of loading of the cutting edges of the mill in the SolidWorks Motion environment which was carried out by graphical modeling of the mill and the workpiece motion. The relative error in determining the cut area by mathematical modeling and simulation was within 1.8 % to 5.7 %.

3. Based on the developed mathematical model, calculation of the cut elements in the arbitrary position of the mill insert on the contact arc was made in the Maple environment. Analysis of influence of the design parameters of the mill and the feed magnitude on the values of the cut elements was done. It was established that the growth of feed caused a linear increase in the chip thickness and width of cut and the depth of cut for the inserts of all steps while the chip thickness had the most intensive growth and the cut depth growth was the least. Growth of the clearance angle from 12 to 20° caused a gradual decrease in the chip thickness, the depth of cut and the main cutting edge angle for the inserts of all steps of the face mill except the fourth step. Also, overload of inserts of the fourth step was observed with a decrease in the angles of slope of the cutting assemblies to 4–5° while the value of the main cutting edge angle exceeded 90°. A growth of these angles to 7–8° caused the transfer of the maximum load to the inserts of the third or second step which is not advisable.

4. With the help of the analysis of loading of the cutting edges, recommendations were formulated for choosing rational design parameters of the face mill for its effective operation at various depths of cuts. For example, at a depth of cut of 3 mm, it is advisable to take the angle of slope of the cutting assemblies equal to 6° and the clearance angle equal to 16°.

References

1. Altintaş Y., Budak E. Analytical Prediction of Stability Lobes in Milling // CIRP Annals. 1995. Vol. 44, Issue 1. P. 357–362. doi: 10.1016/s0007-8506(07)62342-7
2. Euan I. G., Ozturk E., Sims N. D. Modeling Static and Dynamic Cutting Forces and Vibrations for Inserted Ceramic Milling Tools // Procedia CIRP. 2013. Vol. 8. P. 564–569. doi: 10.1016/j.procir.2013.06.151
3. Stepchyn Ya. A. Porivnialna kharakterystyka dynamiky protsesiv tortsevoho frezeruvannia frezamy standartnykh ta spetsialnykh konstruktsiyi // The Journal of Zhytomyr State Technological University. 2015. Issue 1 (72). P. 51–56.
4. Klimenko S. A. Improvement of performance of finishing of details with a cutting tool // The Journal of Zhytomyr State Technological University. 2017. Vol. 2, Issue 2 (80). P. 56–66. doi: 10.26642/tn-2017-2(80)-56-66
5. Hlembotska L. Ye., Melnychuk P. P. Vdoskonalennia protsesu tortsevoho frezeruvannia zahartovanykh stalei: problemy, propozytsiyi, obgruntuvannia // Visnyk ZhDTU. 2010. Issue 2 (53). P. 3–15.
6. Muñoz-Escalona P., Maropoulos P. G. A geometrical model for surface roughness prediction when face milling Al 7075-T7351 with square insert tools // Journal of Manufacturing Systems. 2015. Vol. 36. P. 216–223. doi: 10.1016/j.jmsy.2014.06.011
7. Saï K., Bouzid W. Roughness modeling in up-face milling // The International Journal of Advanced Manufacturing Technology. 2005. Vol. 26, Issue 4. P. 324–329. doi: 10.1007/s00170-004-2305-2
8. Special features in the application of fractal analysis for examining the surface microrelief formed at face milling / Moskvin P., Balytska N., Melnychuk P., Rudnitskyi V., Kyrylovych V. // Eastern-European Journal of Enterprise Technologies. 2017. Vol. 2, Issue 1 (86). P. 9–15. doi: 10.15587/1729-4061.2017.96403

9. Popke H., Emmer T., Alex R. Dynamisch stabile Fräsen mit Schnittaufteilung // Werkstatt und Betrieb: WB (München). 2001. Issue 12 (134). P. 23–29.
10. Karpuschewski B., Batt S. Improvement of dynamic properties in milling by integrated stepped cutting // CIRP Annals. 2007. Vol. 56, Issue 1. P. 85–88. doi: 10.1016/j.cirp.2007.05.001
11. Vyhovskyi H. M., Hromovyi O. A., Melnychuk P. P. Vykorystannia kinematychnykh skhem rizannia pry chystovomu tortsevomu frezeruvanni // Visnyk ZhITI. 2000. Issue 13. P. 18–25.
12. Vyhovskyi H. M., Hromovyi O. A., Melnychuk P. P. Rozrakhunok syl rizannia pry obrobtsi detalei stupinchastymy tortsevymy frezamy // Visnyk ZhITI. 1999. Issue 11. P. 58–66.
13. Vyhovskyi H. M. Kolyvannia syl rizannia pry obrobtsi detalei tortsevymy stupinchastymy frezamy // Visnyk ZhITI. 1998. Issue 9. P. 28–32.
14. Ghorbani H., Moetakef-Imani B. Specific cutting force and cutting condition interaction modeling for round insert face milling operation // The International Journal of Advanced Manufacturing Technology. 2016. Vol. 84, Issue 5-8. P. 1705–1715. doi: 10.1007/s00170-015-7985-2
15. Manohin A. S., Klimenko S. A., Mel'niychuk Yu. A. Parametry secheniya sreza pri tochenii instrumentom s tsilindricheskoy peredney poverhnost'yu // Rezanie i instrument v tekhnologicheskih sistemah. 2010. Issue 78. P. 105–112.
16. Mel'niychuk Yu. A., Klimenko S. A., Manohin A. S. Vliyanie rezhimov obrabotki na sily rezaniya pri tochenii detaley iz zakalenoy stali instrumentom s tsilindricheskoy peredney poverhnost'yu // Nadiyinist instrumentu ta optymizatsiya tekhnolohichnykh system. 2011. Issue 28. P. 39–43.